Astron. Astrophys. 343, 266–272 (1999)

ASTRONOMY AND ASTROPHYSICS

# An investigation of the B335 region through far infrared spectroscopy with ISO⋆

**B. Nisini[1], M. Benedettini[1], T. Giannini[1,2,3], P.E. Clegg[4], A.M. Di Giorgio[1], S.J. Leeks[4], R. Liseau[5], D. Lorenzetti[2], S. Molinari[6], P. Saraceno[1], L. Spinoglio[1], E. Tommasi[7], G.J. White[4], and H.A. Smith[8]**

[1] CNR-Istituto di Fisica dello Spazio Interplanetario, Area di Ricerca Tor Vergata, via Fosso del Cavaliere, I-00133 Roma, Italy
[2] Osservatorio Astronomico di Roma, I-00040 Monteporzio, Italy
[3] Istituto Astronomico, Università "La Sapienza", via Lancisi 29, I-00161 Roma, Italy
[4] Physics Department, Queen Mary and Westfield College, University of London, Mile End Road, London E1 4NS, UK
[5] Stockholm Observatory, S-133 36 Saltsjöbaden, Sweden
[6] Infrared Processing and Analysis Center, Pasadena, CA 91125, USA
[7] Agenzia Spaziale Italiana, via di Villa Patrizi 13, I-00161 Roma, Italy
[8] Harvard-Smithsonian Center for Astrophysics, 60 Garden Street, Cambridge MA, USA

Received 18 May 1998 / Accepted 28 October 1998

**Abstract.** We present far infrared spectra of the B335 dark cloud region, obtained with the Long Wavelength Spectrometer (LWS) on-board the ISO satellite. Deep spectra were obtained towards the far infrared outflow exciting source, located in the B335 core, and on the three associated Herbig Haro (HH) objects HH119 A, B and C. In addition, a region of about 9′ in RA and 4′ in Dec. was mapped which covers the whole molecular outflow.

[CII]158 $\mu$m emission was found to be uniformly distributed across the observed region, with the intensity expected for a photodissociation region excited by the average interstellar field. The [OI]63$\mu$m emission was detected only towards two out of the three HH objects and from the B335 FIR source; excitation from the high-velocity shocks responsible for the HH119 knots can account for the observed line intensity. CO line emission from the rotational levels $J$=15 to $J$=18 was detected only towards B335 FIR and can be modelled as arising in warm gas whose excitation temperature is in the range 150-800 K, located in a compact ($\sim 10^{-3}$ pc) and dense ($n_{H_2} \sim 10^6$ cm$^{-3}$) region. If we assume that the CO $J$ = 6→5 line observed from the ground is also emitted from the same gas component, we derive for this component a temperature of 350 K and a density of $5{\cdot}10^5$ cm$^{-3}$. Current collapse models for the B335 core fail to predict the presence of such warm gas in the infalling source envelope, at the spatial scales implied by our model fit. It is likely that the molecular emission is excited in a low-velocity ($v \sim 10$ km s$^{-1}$) non-dissociative shock, originating at the base of the flow.

**Key words:** stars: formation – ISM: B 335 – ISM: HH 119 – ISM: jets and outflows infrared: ISM: lines and bands

## 1. Introduction

The dark globule B335, located at a distance of 250 pc, appears in the POSS prints as an opaque region extended 2′ EW and 3′ NS (Frerking et al. 1987). It contains a well collimated bipolar outflow oriented almost perpendicular to the line of sight with an estimated dynamical age of about $2{\cdot}10^4$ yr (Moriarty-Schieven et al. 1989, Hirano et al. 1992). The exciting source of the outflow has been identified as a low-luminosity ($L$ = 2.9 $L_\odot$) far-infrared/sub-millimeter object (B335 FIR), associated with the IRAS source IRAS19345+0727 (Chandler et al. 1990), in the centre of a dense core of about 30″ of diameter (Frerking et al. 1987). From the analysis of the profiles of CS and $H_2CO$ lines, Zhou et al.(1990,1993) firstly suggested that the core may still be collapsing. Further evidence for the collapse in B335 has been more recently inferred also by Gregersen et al. (1997) and Mardones et al. (1997).

The small scale structure of the protostellar core has been studied through high resolution observations of $^{12}$CO, other CO isotopomers and millimeter continuum observations (Hirano et al. 1992, Chandler & Sargent 1993). They resolved a condensation of about 10″ diameter, an average density of $\sim 3{\cdot}10^6$ cm$^{-3}$, and total mass of $\sim$ 0.2 $M_\odot$, *i.e.* containing $\sim$ 5% of the total mass of the B335 core.

Three HH objects, HH119A, B and C, have been found in the outflow, and together with the FIR source, are aligned along the outflow axis (Reipurth et al., 1992). HH119 B and C lie at the same distance from the FIR source, in opposite directions, while HH119A lies further away from the source in the red outflow lobe. The morphology and the location of these Herbig-Haro may suggest that the embedded source is undergoing episodic eruptions, which are probably connected with disk-accretion events.

Keene et al. (1983), estimate that the visual extinction is already $>$ 100 mag at a distance of $\sim$ 15″ from the central source; this extremely heavy obscuration prevents any optical

*Send offprint requests to*: B. Nisini (bruni@taurus.ifsi.rm.cnr.it)

⋆ Based on observations with ISO, an ESA project with instruments funded by ESA Member States and with the participation of ISAS and NASA

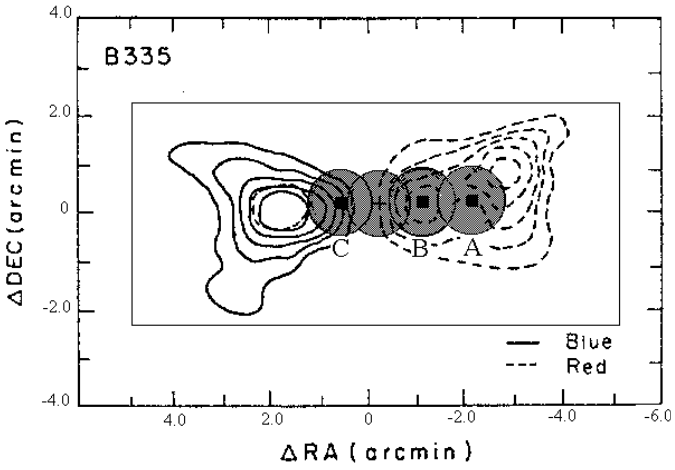


**Fig. 1.** The ISO-LWS pointing positions are superimposed on the CO outflow map in B335 (taken from Goldsmith et al. 1984). The cross and the squares indicate the position of the far-infrared source and of the three HH119 objects (A, B and C) respectively. The rectangular area outlines the region of the raster map.

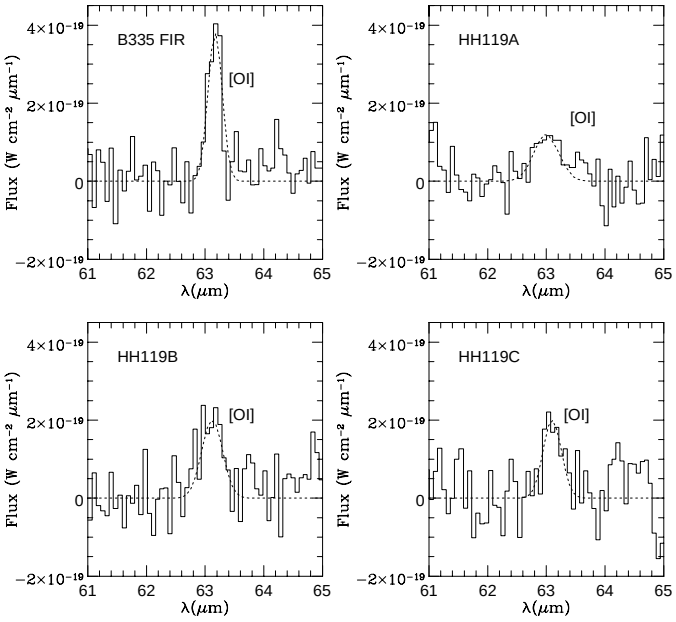


**Fig. 2.** Continuum subtracted [OI]63$\mu m$ line spectra in B335 and in the three HH objects. Dashed line represents the gaussian fit through the data used for deriving the integrated flux.

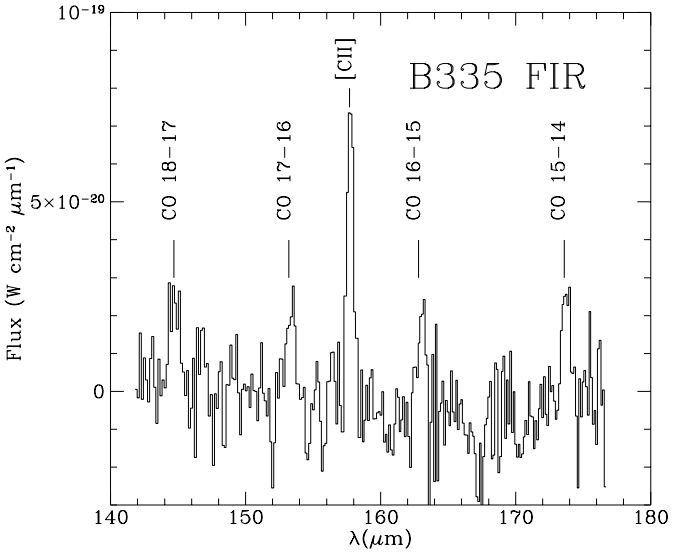


**Fig. 3.** Continuum subtracted LW4 spectrum of B335 which shows the detected CO and [CII]158$\mu m$ lines.

or near infrared observations of phenomena taking place close to the FIR source (IRAS puts only an upper limit of 0.2 Jy at the 25$\mu$m flux density). On the other hand, measurements in the submm/mm/radio, which have been widely used to characterise the properties of the B335 core, are not able to trace the innermost component of warm material and therefore do not probe the heating mechanisms, such as shock interactions due to the outflow or to accretion. Since these may play a fundamental role in understanding the protostellar energy balance and evolutionary state, mid- and far-IR spectroscopic observations are mandatory to probe deeply into the core.

The Long Wavelength Spectrometer (LWS, Clegg. et al. 1996) on the Infrared Space Observatory (ISO, Kessler et al. 1996) allows sensitive spectra to be obtained over the complete spectral range extending from 43 to 197$\mu$m; this wavelength interval contains strong transitions of gaseous species, like $O^o$, $C^+$, CO and $H_2O$, which are the principal species responsible for the cooling in a variety of physical excitation mechanisms, comprising radiative shocks, photodissociation regions and infalling envelopes. It is likely that some, or all of these are present close to the centre of the protostellar core.

## 2. Observations and results

The B335 region was observed with the ISO-LWS operating in its spectroscopic grating mode (covering the interval 43-196.7$\mu$m at a resolution of $\sim 200$ and with an average beamsize of about 80″), during revolutions 181 and 316. Grating spectra were obtained of B335 FIR ($19^h\ 34^m\ 35.3^s$ $+07^o\ 27'\ 24''$, B1950), and the three HH objects 119A, B and C, integrating for 40 s at each spectral element, with a total on-target time of 4450 s. In addition, a raster map was made covering 7×3 LWS beams spaced 80″ from each other, centered on the FIR source (see Fig. 1). Each raster point was integrated for 6.4 s per spectral element (714 s on-target time). All the spectra were oversampled by a factor 4 and were calibrated using observations of Uranus with an estimated accuracy better than 30% (Swinyard et al. 1996).

The data were processed with the LWS Pipeline Version 6.0; additional analysis included removal of spurious signals due to cosmic ray impacts and averaging the grating scans of each detector. Figs. 2, 3 and 4 show the continuum subtracted (by second order polynomial fitting) portions of the spectra from which lines were detected. The continuum in the HH objects and in the raster map positions is negligible, while on B335 FIR

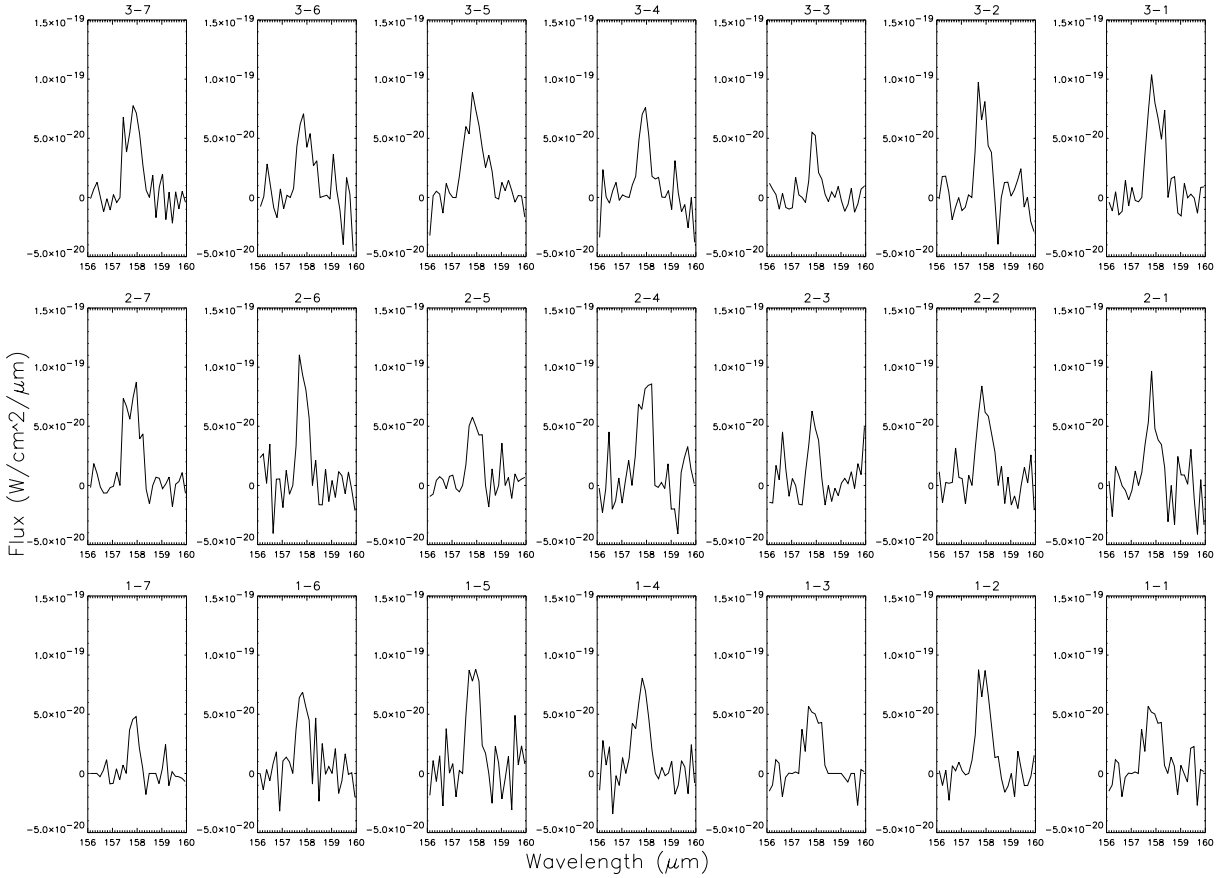


**Fig. 4.** [CII] line emission in the 7x3 raster map. The central position (2-4) corresponds to B335 FIR, and the spatial step is 80″.

**Table 1.** Observed line fluxes in B335 FIR

| $\lambda_{vac}$ ($\mu$m) | Line id. | $\lambda_{obs}$ ($\mu$m) | F ($10^{-20}$ W cm$^{-2}$) | $\Delta$F |
|---|---|---|---|---|
| 63.18 | [OI] $^3P_1 \rightarrow {}^3P_2$ | 63.18 | 9.4 | 1.7 |
| 130.37 | CO 20-19 | ... | <1.2 | 3$\sigma$ u.l. |
| 137.20 | CO 19-18 | ... | <1.5 | 3$\sigma$ u.l. |
| 144.78 | CO 18-17 | 144.66 | 1.4 | 0.3 |
| 153.27 | CO 17-16 | 153.46 | 2.2 | 0.5 |
| 157.74 | [CII] $^2P_{3/2} \rightarrow {}^2P_{1/2}$ | 157.82 | 4.8 | 0.4 |
| 162.81 | CO 16-15 | 163.00 | 2.0 | 0.3 |
| 173.63 | CO 15-14 | 173.66 | 1.5 | 0.4 |
| 186.00 | CO 14-13 | ... | <3.7 | 3$\sigma$ u.l. |

**Table 2.** Observed line fluxes in the HH119 objects

| $\lambda_{vac}$ ($\mu$m) | Line id. | $\lambda_{obs}$ ($\mu$m) | F ($10^{-20}$ W cm$^{-2}$) | $\Delta$F |
|---|---|---|---|---|
| **HH119 A** | | | | |
| 63.18 | [OI] $^3P_1 \rightarrow {}^3P_2$ | 63.11 | <4.5 | 3$\sigma$ u.l. |
| 157.74 | [CII] $^2P_{3/2} \rightarrow {}^2P_{1/2}$ | 157.83 | 4.6 | 0.4 |
| **HH119 B** | | | | |
| 63.18 | [OI] $^3P_1 \rightarrow {}^3P_2$ | 63.20 | 6.3 | 1.8 |
| 157.74 | [CII] $^2P_{3/2} \rightarrow {}^2P_{1/2}$ | 157.77 | 3.8 | 0.2 |
| **HH119 C** | | | | |
| 63.18 | [OI] $^3P_1 \rightarrow {}^3P_2$ | 63.10 | 5.4 | 1.7 |
| 157.74 | [CII] $^2P_{3/2} \rightarrow {}^2P_{1/2}$ | 157.70 | 4.8 | 0.4 |

the observed line to continuum ratios range from 0.5 at 63$\mu$m to $\sim 5{\cdot}10^{-2}$ for the lines measured from 140 to 180$\mu$m.

Tables 1 and 2 summarise the results of the observations. The line fluxes were computed by gaussian fitting the spectral profiles, which always had an FWHM comparable with the instrumental resolution element width (*i.e.* 0.29 and 0.60 $\mu$m for the SW and LW detectors respectively). The reported errors refer to the statistical errors obtained from the residual of the gaussian fit with respect to a local baseline; they are always less or comparable to the calibration errors.

Towards B335 FIR we detected emission from [OI]63$\mu m$, [CII]158$\mu m$ and from four CO transitions with rotational numbers $J_{up}$ = 15, 16, 17 and 18. All the HH objects present the [CII]158$\mu m$ line, while a clear detection (at more than three $\sigma$) of the [OI]63$\mu m$ is obtained only towards HH119 B and C (Figs. 2 and 3). In the raster map positions, only [CII] was detected. The spectra were also co-added in order to search for diffuse emission in the [OI]63$\mu m$ line, resulting in a 3$\sigma$ upper

limit of $3{\cdot}10^{-20}$ W cm$^{-2}$. In Fig. 4 the [CII] spectra are shown at all the map positions. The [CII] line flux in the position centered on B335 FIR is consistent with the value measured in the pointed observation, which was performed about 130 revolutions earlier, indicating the stability of the measurement procedure.

## 3. Discussion

### *3.1. The [CII]158$\mu m$ diffuse emission*

The spectra from the raster map (Fig. 4) show that the [CII]158 $\mu m$ line intensity remains very uniform across the mapped region. Given the associated uncertainties, all of the positions have comparable flux levels, with an average value of $[4.7{\pm}0.4]{\cdot}10^{-20}$ W cm$^{-2}$. Considering that the LWS beamwidth at 150$\mu$m is about 80″, the observed flux corresponds to a diffuse line intensity of $2.4{\cdot}10^{-6}$ erg s$^{-1}$ cm$^{-2}$ sr$^{-1}$. Such diffuse and uniform emission is expected to originate in a photodissociation region (PDR) resulting from illumination of material by a weak interstellar field. For a PDR exposed to such a low FUV flux, and having densities $< 10^4$ cm$^{-3}$ (such as those measured in the investigated region, Frerking et al. 1987), it is expected that $I_{158\mu m} \sim 10^{-6} \times G_0$ erg s$^{-1}$ cm$^{-2}$ sr$^{-1}$, where $G_0$ is the FUV flux measured in units of $1.6{\cdot}10^{-3}$ erg s$^{-1}$ cm$^{-2}$ (Hollenbach et al. 1991); this relationship indicates that the observed intensity is consistent with a FUV field of only 2 - 3 $G_0$. In these conditions the expected [OI] 63$\mu$m emission should be $\sim 10^{-9}$erg s$^{-1}$ cm$^{-2}$ sr$^{-1}$, consistent with the observed upper limit of $2{\cdot}10^{-6}$erg s$^{-1}$ cm$^{-2}$ sr$^{-1}$. No increase of [CII] on the FIR source was observed, implying the absence of a PDR excess close to the central object, as expected given the low luminosity of the source.

### *3.2. The HH objects*

HH119B and C have comparable [OI]63$\mu$m line fluxes considering the associated errors (see Table 2). The upper limit towards HH119A does not exclude that here the 63$\mu$m line has a similar value than in the other observed knots. In order to understand if this emission could originate from the outflow material, the seven map spectra located along the flow axis were averaged together. No significant line emission was detected in the resulting spectrum indicating that almost all the [OI] is confined to the region covered by the pointed observations. Since this localised emission is not originated from the diffuse PDR responsible for the [CII], it has to be entirely due to shock excitation. It is therefore reasonable to assume that it is excited by the same shocks responsible for the HH knots which are expected to be high velocity (the knots are travelling at velocities of the order of 200 km s$^{-1}$), dissociative shocks. Of the three HH objects, knot A (see Fig. 1) has the higher excitation spectrum and exhibits a bow-shock morphology, while knot B appears to be less excited and it is located closer to the star where the medium has probably already been compressed by the passage of the first shock (Reipurth et al., 1992). Such a difference in excitation is not apparent in the 63$\mu$m emission, which, as already noticed, has at least a similar flux level in both the objects.

According to Hollenbach & McKee (1989), the 63$\mu m$ intensity originating from a high velocity dissociative shock ("J" type shock) is:

$$I_{63\mu m} \sim 10^{-13} \cdot n_o \cdot v_s \; erg \; cm^{-2} \; s^{-1} \; sr^{-1}, \quad (1)$$

where $v_s$ is the shock velocity and $n_o$ is the pre-shock density.

This latter is defined as the density of the medium before the passage of the shock, and can therefore be taken equal to the ambient density, estimated to be $\sim 3{\cdot}10^3$ cm$^{-3}$ at distances in the range 0.07 to 0.2 pc from the FIR source (Frerking et al., 1987). Assuming that the shock velocity is similar to the velocity at which the three HH objects are travelling, the [OI] intensity should be $\sim 6{\cdot}10^{-3}$ erg s$^{-1}$ cm$^{-2}$ sr$^{-1}$, which, compared with the observed flux density, indicates that the region from which the emission originates can be no more than a few arcsec across, *i.e.* comparable with the size of the optical knots.

This result also implies that, in the region of the outflow covered by the three measurements considered here, the optical HH objects are the only shocked knots present, since the estimated emission sizes of the 63$\mu$m line exclude the presence of additional, heavily extincted, and thus visually not observed, shock excited regions.

### *3.3. B335 FIR*

#### 3.3.1. [OI] emission

The [OI] flux observed in the spectrum of B335 FIR is only slightly greater than that observed towards the HH objects (by less than a factor of two). Since the HH knots are probably related to episodic eruptions from the embedded source (Reipurth et al, 1992), this emission could in principle originate in an inner shock due to a more recent outburst, which has not been observed at optical wavelengths due to the high extinction close to the source.

Given the linear dependence of the [OI] line intensity on the ambient density, the relatively higher flux could be explained by an increase of the density closer to the dense core. Indeed, according to the density gradients derived by Frerking et al. (1997), the $n_{\rm H_2}$ may steepen at distances of $\sim 0.05$ pc from the central source.

Alternatively, the [OI] emission could be also due to a lower velocity shock originating when the jet obliquely impacts the dense core in which the source is embedded. This hypothesis will be more carefully analyzed in the next section, in connection with the analysis of the CO line emission.

The possibility has also been considered that the [OI] emission originates from material in the infalling envelope surrounding B335 FIR. The observed 63$\mu$m luminosity, at the distance of 250 pc, is $1.8{\cdot}10^{-3}$ L$_\odot$: Zhou et al. (1990,1993) model the FIR source as a protostar of $\sim 0.4$ M$_\odot$ with an accretion rate of $2.8{\cdot}10^{-6}$ M$_\odot$ yr$^{-1}$. Assuming these parameters and following the model by Ceccarelli et al. (1996) for the line cooling in collapsing envelopes, the expected [OI] luminosity should be a factor three lower than observed. Models for accretion shocks in protostellar disks (Neufeld and Hollenbach, 1994), predict that the 63$\mu$m luminosity should be even lower. Considering

also the calibration errors affecting the 63$\mu$m flux, we can say that the release of the gravitational energy due to infall could in principle contribute up to half of the observed luminosity.

In conclusion, it is not easy to define, by means of the [OI] line flux only, if there is a single prevailing mechanism for the excitation of this line towards B335 FIR. More constrains can be obtained by the analysis of also the CO lines.

### 3.3.2. CO emission

To understand the origin of the observed high-$J$ CO rotational lines, it is necessary to estimate the physical parameters which characterise this gas component. For that, a Large Velocity Gradient code with a plane-parallel geometry was used. In this model, the CO collisional downward rates for levels with $J_{up} <$ 60 and $T >$ 100 K were calculated using the $\gamma_{J0}$ coefficients taken from McKee et al.(1982), while the upward rates were computed using the principle of detailed balance, and radiative decay rates were taken from Chackerian & Tipping (1983). An intrinsic line-width of 10 km s$^{-1}$ has been used, equal to the maximum velocity observed in the extended CO outflow: the validity of this assumption will be discussed later.

The model depends on several other free-parameters (temperature, density, filling factor and depth of the emitting region) some of which are related together. The relatively high uncertainty in the line flux determination is sufficient only to allow a range of possible physical conditions to be given which are compatible with the observations. In particular, from the ratios of the lines observed by the LWS and their associated errors, a range of possible excitation temperatures and densities can be derived, which span from 150-800 K and $5{\cdot}10^5$-$4{\cdot}10^6$ cm$^{-3}$ respectively (see Table 4 and Fig. 5). We remark that this range of parameters is compatible with the statistical errors reported in Table 1, which are the appropriate uncertainties to be applied to the *ratios* of lines detected by the same detector, as in this case.

We can see if the derived physical parameters can be better constrained by using also available ground-based observations. In particular, the CO $J$=6→5 line towards the FIR source has been observed by Graf et al. (1993) at the JCMT, with a beam of 8″. If we assume that the 6→5 emission comes from the same region of the lines observed by the LWS, we can rather uniquely define a model fit consistent with all the observations, having a temperature of 350 K and a density of $5{\cdot}10^5$ cm$^{-3}$ (see Fig. 5). In this model, the line optical depths are of the order of unity, and imply a CO column density of $1{\cdot}10^{18}$ cm$^{-2}$: given this, the size of the emitting gas can be estimated from the absolute line flux, and results to be of the order of 1.5″ ($2{\cdot}10^{-3}$ pc at 250 pc). We stress, however, that since Graf et al. did not map the region around B335 FIR covered by the LWS beam, the possibility that the 6→5 emission is in fact originated by a region larger than the one implied by the LWS high-$J$ observations cannot be excluded. In particular, some, if not most, of the 6→5 emission could be indeed associated with the large scale outflowing gas having a much lower temperature of about 10-30 K. The above analysis indicates anyhow the presence of a warm CO component emitting from a dense and compact region with a total luminosity of about $10^{-3}$ of the stellar luminosity and about double the luminosity due to [OI] in the same spectrum (*i.e.* $1.8{\cdot}10^{-3}$ L$_\odot$).

Where does the warm gas come from? We first investigated if it could originate in the collapsing envelope modelled for B335 by Zhou et al. (1993). Our derived density range in a region of diameter about $6{\cdot}10^{15}$ cm is consistent with the average density implied by the Zhou et al. density distribution inside the collapsing radius. However, in these circumstances the gas temperature would remain very low ($<$ 30 K) inside the envelope, in contradiction with the presence of the warm CO gas we are probing here. This result has been also confirmed by Hartstein & Liseau (1998), who made specific predictions on the expected CO emission from B335 FIR assuming a Shu-type infall; they found that the contribution from the infalling envelope in the high-$J$ CO lines is several orders of magnitude less than observed by the LWS.

**Table 4.** Physical parameters of the CO emission

| | (1) | (2) | (3) |
|---|---|---|---|
| Gas temperature $T$ (K) | 350 | 150 | 800 |
| Gas density $n_{\rm H_2}$ (cm$^{-3}$) | $5{\cdot}10^5$ | $4{\cdot}10^6$ | $5{\cdot}10^5$ |
| CO column density $N_{\rm CO}$ (cm$^{-2}$) | $1{\cdot}10^{18}$ | $4{\cdot}10^{18}$ | $1{\cdot}10^{17}$ |
| Size (″) | 1.5 | 2 | 1 |
| Size (pc) | 0.002 | 0.002 | 0.001 |
| CO cooling $L_{\rm CO}$ (L$_\odot$) | 0.004 | 0.003 | 0.005 |

(1): best fit obtained with both LWS and JCMT observations.
(2), (3): extreme model fits which are consistent with only the LWS observations (see text).

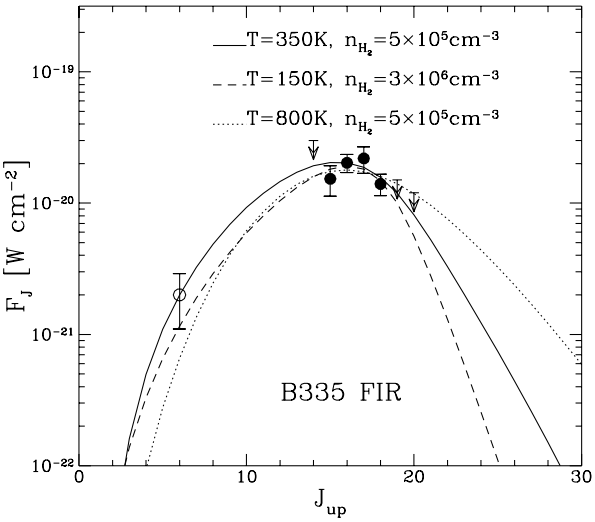


**Fig. 5.** Model fit of the observed CO line fluxes. In addition to the high-$J$ rotational lines observed by the LWS (filled dots), also the CO 6→5 line from Graf et al. (1993) is reported (open dot). The solid line indicates the best fit obtained taking into account both the LWS and the CO 6→5 observations, while dotted and dashed lines represent respectively the coldest and warmest model fits derived from the LWS data only.

If the CO emission does not come from the collapsing envelope, it could originate in high velocity shocks responsible for the HH presence. In high velocity J-type shocks, molecules are dissociated at the shock front and then are able to reform and contribute significantly to the cooling further away in the post-shock region, when the temperature has dropped to $\lesssim$ 500 K (Hollenbach & McKee 1989). In contrast, [OI] will already contribute significantly to the cooling at temperatures $\sim$ 5000 K, its emission coming from a larger fraction of the volume of the post-shock region. Both the CO temperature and the size of the emitting region we have estimated (which must be at least half of the estimated size of the [OI] emission) would agree with such a picture. However, the derived CO luminosity exceeds that of the [OI]63$\mu$m line; a situation which should happen only in very dense J-shocks, *i.e.* where the pre-shock density exceeds $10^5$ cm$^{-3}$ (Hollenbach & McKee 1989). The total luminosity radiated by such a fast and dense shock would be:

$$L_{rad} = \frac{1}{2}\mu m_{\rm H} \cdot n_o \cdot v_s^3 \cdot A_{eff}. \quad (2)$$

Taking a pre-shock density $n_o > 10^5$ cm$^{-3}$ and an effective shock area $A_{eff}$ corresponding to the estimated size of the emitting region ($\sim 10^{-3}$ pc), then $L_{rad} > 15$ L$_\odot$, *i.e.* $> 10^3$ times the luminosity radiated by the observed FIR lines and more than 5 times the luminosity of the central source ! In addition, we also note that a pre-shock density $> 10^5$ cm$^{-3}$ also contrasts with the estimated *post*-shock density ($\sim 5{\cdot}10^5$ cm$^{-3}$) since, according to Hollenbach & McKee (1989), the compression factor for shocks with velocities larger than 100 km s$^{-1}$ and magnetic fields less than 1 mG, which is the upper limit derived towards B335 (Rydbeck et al. 1980), is expected to be greater than at least 20.

It is more likely that the observed CO emission comes from a different and non-dissociative shock component having a lower velocity (*i.e.* from a "C" shock): since in C-shocks the peak temperature of the postshock gas is directly related to the shock velocity, our estimated gas temperature $\sim$ 350 K can be translated to an estimated velocity $\sim$10 km s$^{-1}$ (Kaufman & Neufeld 1996). The presence of slow shocks connected with outflow activity in YSOs has already been inferred in a variety of different sources (Nisini et al. 1998, Ceccarelli et al. 1998, Liseau et al. 1996). A more detailed comparison of the observed emission with the Kaufman & Neufeld models favours a shock with $v_s \sim$ 10km s$^{-1}$ and $n_{\rm o} \sim 10^5$ cm$^{-3}$. The total luminosity radiated by this shock is, adopting the relationship given in Eq. (2), $\sim$ 0.005 L$_\odot$, *i.e.* comparable to the total luminosity of the CO emission. In such a model, CO is indeed expected to be the major coolant of the shocked gas, since the contribution at the cooling of $H_2O$ lines is still not dominant in slow ($<$ 15 km s$^{-1}$) shocks, where the temperature is not high enough to trigger the endothermic reactions which bring all the free atomic oxygen into water (Bergin et al. 1998, Kaufman & Neufield 1996). On the other hand, if oxygen is not converted into water, it should also contribute at the shock cooling, so one could argue that the observed [OI]63$\mu$m emission is also due to the same low velocity shock responsible for the CO emission. Given the high column density estimated from the CO lines analysis (which, assuming a standard CO/$H_2$ abundance of $10^{-4}$ correspond to a $H_2$ column density greater than $10^{21}$ cm$^{-2}$), the 63$\mu$m line would be expected to be optically thick for the considered temperature range, if all the oxygen is indeed present in its atomic form. Assuming an emission size of about 0.002 pc and a linewidth of 10 km s$^{-1}$, we have that the contribution of the 63$\mu$m line to the considered shock should be about $8{\cdot}10^{-19}$ W cm$^{-2}$, *i.e.* significantly larger than the flux we are actually observing. We should however keep in mind that part or most of the oxygen could be in other molecules like $O_2$ or even depleted on grains (e.g. van Dishoeck et al. 1993, Bergin et al. 1995), thus making this estimation just an upper limit of the possible [OI] contribution. We can therefore only conclude that the observed 63$\mu$m emission is not in contradiction with the presence of the considered low velocity shock.

The contribution of $H_2$ pure rotational lines is also predicted to be less than 30% of the CO luminosity, while such a slow shock would not be expected to emit strongly in the near-infrared rovibrational $H_2$ lines, since they all have excitation temperatures above 1000 K. Indeed, images in the 1-0 S(1) line at 2.12$\mu$m obtained at the European Southern Observatory (Nisini, unpublished data) do not show diffuse emission from $H_2$ at a level of $\sim 10^{-5}$ erg s$^{-1}$ cm$^{-2}$ sr$^{-1}$.

We finally comment about the fact that we find broad agreement with the Kaufman & Neufield C-shock model despite that the actual shock we are observing is probably neither planar nor stationary as the model assumes. Given however the spatial and temporal averaged physical quantities that we can infer by our observations a detailed comparison with more specific models would be impossible.

### *3.4. Discussion on the different shock components*

The analysis of the far infrared lines towards B335 FIR indicates the presence of both high and low velocity shock components along the flow excited by the infrared source. The occurrence of shocks at different velocities and having different excitation conditions is common along molecular outflows as evident by the simultaneous presence of HH objects (characteristics of dissociative shock interactions) and emission from molecular hydrogen, which does not survive in shocks with velocities greater than $\sim$ 50 km s$^{-1}$. Models for the origin of bipolar outflows predict the formation of a wide range of shock conditions. In outflows triggered by collimated stellar jets (Chernin & Masson 1995, Raga & Cabrit 1993) a bow shock is created at the head of the jet, with the highest velocities occurring along the flow axis and progressively slower shocks along the bow tails. In outflows driven by wide-angle collimated winds (Shu et al. 1995), the highest velocities should occur when it strikes the ambient medium at the maximum speed, and the slower shocks would then lie further back where the wind obliquely impacts on the surrounding medium.

The low spatial and spectral resolution of the LWS data do not allow discrimination between the different possibilities

but the derived general characteristcs of the far infrared line emission do not contradict any of the above scenarios.

The integrated luminosity from [OI] and CO observed along the outflow is $\sim 10^{-2}$ $L_{\odot}$, which is comparable with the outflow kinetic luminosity ($4{\cdot}10^{-2}$ $L_{\odot}$, Hirano et al. 1992). This is indeed what is expected if the shocks traced by the FIR lines are accelerating the ambient medium into the molecular outflow (Davis & Eislöffel 1995), further supporting the close association of the observed line emission with the mechanism driving the outflow, whether it is a jet or a collimated wind.

Finally, we note that the CO emission, unlike that of [OI], is observed only towards the central source and not along the outflow. The CO lines detected on-source however have a lower signal to noise ratio; shocks at lower densities such as those which could be originated along the flow, would probably produce a column density of warm CO too low for the detection of the molecular lines with the LWS.

## 4. Conclusions

A region of about $9' \times 4'$around the FIR source in the center of the B335 core, has been investigated with the LWS full grating spectroscopic observations over the 43-197$\mu$m range, with the following results:

- a diffuse and uniform emission from [CII] is present over the whole region with an intensity which can be accounted for by a weak interstellar FUV field of about 2-3 $G_o$.
- emission from [OI] was only detected in the pointed observations towards the FIR source and the two Herbig Haro objects HH119B and C. The high-velocity (v$\sim$200 km s$^{-1}$) shock interactions responsible for the Herbig-Haro objects can account for the [OI] line intensity detected towards the HH knots.
- CO emission from the rotational levels $J$=15 to $J$=18 was detected only in the direction of the FIR source; the analysis of these lines suggests that they arise in a dense ($n > 10^5$ cm$^{-3}$) and compact ($\sim 10^{-3}$) region and have excitation temperatures in the range from 150 to 800 K. If we also assume that the line emission from the $J$=6 level, observed from the ground, originates from the same component, we derive that a gas at a density of $5{\cdot}10^5$ cm$^{-3}$ and a temperature of 350 K can accounts for both the LWS and ground-based observations. From the estimated characteristics of the excitation conditions we conclude that a different shock component, at much lower velocities, should be responsible for the excitation of these lines.
- Such a slow shock could also be responsible for the observed [OI] emission towards the FIR source, in which case we derive that only a fraction of the oxygen is available in the atomic form. Alternatively the [OI] emission could originates in a high velocity shock, similar to the ones observed on the HH objects, and due to a more recent and still embedded outburst.
- The total integrated luminosity from the [OI] and CO lines is comparable with the kinetic luminosity of the bipolar outflow associated with B335 FIR, indicating the connection of the observed lines with the mechanism driving the outflow.
- We also derive that the CO emission cannot be taken into account by the energy release during accretion, since current models for infalling envelopes predict that the cooling in FIR lines from this low-luminosity protostar is much lower than what we observe. Moreover, based on the analysis of the properties of the shocks present in the considered region, we conclude that, although the protostellar collapse could in principle be responsible for part of the [OI] emission, it is not the main excitation mechanism for the observed 63$\mu$m line.

*Acknowledgements.* We would like to acknowledge C. Ceccarelli for running her protostellar collapse code in the case of B335 FIR. We are also grateful to M. Kaufman for having provided us with his C-shock code results. SJL acknowledges receipt of a PPARC award.

## References

Bergin E.A., Langer W.D., Goldsmith P.F., 1995, ApJ 441, 222
Bergin E.A., Melnick G.J., Neufeld D.A., 1998, ApJ 499, 777
Ceccarelli C., Hollenbach D.J., Tielens A.G.G.M., 1996, ApJ 471, 400
Ceccarelli C., Caux E., White G.J., et al., 1998, A&A 331, L17
Chackerian C., Tipping R.H., 1983, J. of Molecular Spectroscopy 99, 431
Chandler C.J., Sargent A.I., 1993, ApJ 414, L29
Chandler C.J., Gear W.K., Sandell G., et al., 1990, MNRAS 243, 330
Chernin L., Masson C., 1995, ApJ 443, 181
Clegg P.E., Ade P.A.R., Armand C., et al., 1996, A&A 315, L38
Davis C.J., Eislöffel J., 1995, A&A 300, 851
Frerking M.A., Langer W.D., Wilson R.W., 1987, ApJ 313, 320
Goldsmith P.F., Snell R.L., Hemeon-Heyer M., Langer W.D., 1984, ApJ 286, 599
Graf U.U., Eckart A., Genzel R., et al., 1993, ApJ 405, 249
Gregersen E.M., Evans N.J., Zhou S., Choi M., 1997, ApJ 484, 246
Hartstein D., Liseau R., 1998, In: Star Formation with the Infrared Space Observatory. ASP Conference Series vol. 132
Hirano N., Kameya O., Kasuga T., Umemoto Y., 1992, ApJ 390, L85
Hollenbach D., McKee C.F. 1989, ApJ 342, 306
Hollenbach D., Takahashi T., Tielens A.G.G.M., 1991, ApJ 377, 192
Kaufman M.J., Neufeld D.A., 1996, ApJ 456, 250
Keene J., Davidson J.A., Harper D.A., et al., 1983, ApJ 274, L43
Kessler M.F., Steinz J.A., Anderegg M.E., et al., 1996, A&A 315, L27
Liseau R., Ceccarelli C., Larsson B., et al., 1996, A&A 315, L181
Mardones D., Myers P.C., Tafalla M., et al., 1997, ApJ 489, 719
McKee C.F., Storey J.W.V., Watson D.M., Green S., 1982, ApJ 259, 647
Moriarty-Schieven G.H., Snell R.L., 1989, ApJ 338, 952
Neufeld D.A., Hollenbach D.J., 1994, ApJ 428, 170
Nisini B., Giannini T., Molinari S., et al., 1998, Star Formation with the Infrared Space Observatory. ASP Conference Series vol. 132
Raga A., Cabrit S., 1993, A&A 278, 267
Reipurth B., Heathcote S., Vrba F., 1992, A&A 256, 225
Rydbeck O.E.H., Irvine W.M., Hjalmarson H.A., et al., 1980, ApJ 235, L171
Shu F.H., Najita J., Ostriker E., Shang S., 1995, ApJ, L155
Swinyard B.M., Clegg P.E., Ade P.A.R., et al., 1996, A&A 315, L43
van Dishoeck E.F., Blake G.A., Draine B.T., Lunine J.I., 1993, In: Levy E.H., Lunine J.H., Protostar and Planets III. Univ. Arizona Press, Tucson, p. 163
Zhou S., Evans N.J., Kömpe C., Walmsley C.M., 1993, ApJ 404, 232
Zhou S., Evans N.J., Butner H.M., et al.,1990, ApJ 363, 168